

Action Prediction Based on Anticipatory Brain Potentials during Simulated Driving

Zahra Khaliliardali*, Ricardo Chavarriaga*, Lucian Andrei Gheorghe * **, and José del R. Millán*

* Defitech Chair in Brain-Machine Interface, Center for Neuroprosthetics, Institute of Bioengineering and School of Engineering, École Polytechnique Fédérale de Lausanne (EPFL), Campus Biotech H4, 1202, Geneva, Switzerland.

** Nissan Motor Co., Ltd. Research Division, Research Planning Department, Atsugi, Japan.

E-mail: zahra.khaliliardali@epfl.ch

Abstract

Objective. The ability of an automobile to infer the driver's upcoming actions directly from neural signals could enrich the interaction of the car with its driver. Intelligent vehicles fitted with an on-board brain-computer interface (BCI) able to decode the driver's intentions can use this information to improve the driving experience. In this study we investigate the neural signatures of anticipation of specific actions, namely braking and accelerating. *Approach.* We investigated anticipatory slow cortical potentials (SCPs) in electroencephalogram (EEG) recorded from 18 healthy participants in a driving simulator using a variant of the contingent negative variation (CNV) paradigm with *Go* and *No-go* conditions: count-down numbers followed by 'Start'/'Stop' cue. We report decoding performance before the action onset using a quadratic discriminant analysis (QDA) classifier based on temporal features. *Main Results.* (i) Despite the visual and driving related cognitive distractions, we show the presence of anticipatory event related potentials locked to the stimuli onset similar to the widely reported CNV signal (with an average peak value of $-8 \mu\text{V}$ at electrode Cz). (ii) We demonstrate the discrimination between cases requiring to perform an action upon imperative subsequent stimulus (*Go* condition, e.g. a 'Red' traffic light) versus events that do not require such action (*No-go* condition; e.g. a 'Yellow' light); with an average single trial classification performance of 0.83 ± 0.13 for braking and 0.79 ± 0.12 for accelerating (area under the curve). (iii) We show that the centro-medial anticipatory potentials are observed as early as 320 ± 200 ms before the action with a detection rate of 0.77 ± 0.12 in offline analysis. *Significance.* We show for the first time the feasibility of predicting the driver's intention through decoding anticipatory related potentials during simulated car driving with high recognition rates.

36 **Keywords:** BCI; Anticipation ; EEG; CNV; Intention detection; Car simulator;
37 SCP.

38 1. Introduction

39 Car drivers are constantly involved in anticipatory and preparatory tasks prompted
40 by processes that can be either internal (endogenous) or triggered by cues from the
41 environment (exogenous). Brain-computer interface (BCI) systems can potentially be
42 used to recognize the driver's intention for a movement such as pressing pedals, or
43 turning left or right before any overt action is performed. Predicting the driver's will
44 can help the driving assistance system of an intelligent car to provide support that is not
45 only in-line with the situations on the road (based on the in-car sensors), but also and
46 more importantly, aligned with the driver's intention (mediated by the driver's BCI).
47 This will ensure a seamless interaction between the car and the driver.

48 To date, studies on monitoring the driver's brain state have mainly focused on the
49 driver's drowsiness/arousal using a combination of Electroencephalogram (EEG) and
50 electrooculogram (EOG) signals [1, 2]. EEG-based systems have been also employed
51 for the detection of driver's workload [2, 3]. Haufe et al. [4] explored the detection of
52 emergency braking before the action onset using EEG and electromyography (EMG).
53 The results of this offline study indicate that the driver's intention to perform emergency
54 braking can be detected as early as 130 ms before the car pedal responses . More recently,
55 they assessed the applicability of their system in real-world driving [5] replicating the
56 findings obtained with the car simulator [4]. Kim et al. [6] have extended these findings
57 in different simulated driving situations, and were also capable to different emergency
58 braking from normal braking.

59 In this work, we investigate the prediction of driver's action based on the decoding
60 of anticipatory brain potentials. Anticipation generates an endogenous pre-activation of
61 underlying neural structures, during which a person actively engages in a preparatory
62 phase after a warning stimulus, in order to execute a specific action after a relevant
63 imperative stimulus [7]. An example in the driving scenario is the color changes of a
64 traffic light, when the traffic light is turning from 'Green' to 'Yellow' to 'Red'. In this
65 case, 'Yellow' is the warning stimulus, as it does not require any mandatory action and
66 simply predicts the appearance of the imperative stimulus 'Red', upon whose appearance
67 the subject is supposed to brake immediately. Therefore, we evaluate the feasibility of
68 predicting the movement onset (e.g. pressing the brake pedal) through anticipatory
69 brain potentials. This will be beneficial in scenarios where the driver is engaged by
70 external events for which he/she needs to perform an immediate action (e.g. 'Red'
71 light) in contrast to occasions where there is no need for an immediate response (e.g.
72 'Yellow' light).

73 As an example of how a BCI based on anticipatory brain potentials can enhance
74 driving, consider a junction with a traffic light turning 'Red'. Two cases might happen.
75 (i) For an inattentive driver who is not aware of the need to brake, the BCI does

76 not detect the presence of anticipation-related potential. Then, the driving assistance
77 generates a warning feedback to the driver while it also initiates the braking action
78 smoothly, so that the driver has the time to become aware of the situation and finish
79 braking the car by him/herself. This kind of driving assistance would prevent an
80 automatic emergency braking at the last moment, which may result in a negative surprise
81 and unpleasant experience for the driver who could feel under the control of the smart car
82 rather than controlling it. (ii) If the driver is aware of the turning traffic light and has the
83 intention to brake, the BCI detects the presence of a CNV and an automatic braking
84 is unnecessary. Still, further driving assistance could be also provided by facilitating
85 the driver's intended action (i.e. initiating the braking action smoothly). We believe
86 that a smart car endowed with a such BCI will lead to a more pleasant and seamless
87 interaction between the two as its driving assistance will always be in accord with the
88 driver's intention. It is worth noting that, the real-time information about the presence
89 and status of a traffic lights can be detected by the embedded sensors in the car [8, 9]
90 which could be transferred to the proposed BCI system. Furthermore, the advent of
91 autonomous cars is accelerating the use of communication networks among cars and
92 key traffic elements, such as traffic lights, that will provide an intelligent car with the
93 necessary information about the status of traffic and other vehicles on the road.

94 In the standard paradigms for studying anticipatory processes, a first warning
95 stimulus (S1) predicts the appearance of second imperative stimulus (S2), signaling
96 that the user has to perform a specific action. A central negative deflection has been
97 observed in the scalp EEG during the interval between the warning (S1) and imperative
98 stimuli (S2) [7]. This signal, termed Contingent negative variation (CNV) potential,
99 develops during most of the inter-stimulus interval and can last from about 300 ms to
100 several seconds with magnitudes up to $50 \mu\text{V}$. Generally, the negativity ends sharply with
101 the onset of Go cue. This potential is linked to the preparatory processing required for
102 appropriate actions at the arrival of future events [7, 10, 11]. Interestingly, recent studies
103 have shown the possibility of detecting similar potentials in complex experimental set-
104 ups that involve a simulated tele-presence robot [12] or operation of Internet browsers
105 [13].

106 Recently, Garipelli et al. [13] studied offline the anticipation-related brain signals
107 and highlighted the advantages of using weighted average spatial smoothing filters
108 and removal of the infra-slow oscillations (below 0.1 Hz). However, the single-trial
109 analysis results of this study were confined only to synchronous classification. Similar
110 preprocessing methods have been proposed for the detection of movement intention
111 through slow Movement-related cortical potentials (MRCs) or Readiness potentials
112 (RPs) pointing to similar frequency ranges. Both CNVs and MRCs result in a similar
113 deflections in the slow brain potentials of EEG called Slow cortical potentials (SCPs).
114 SCs are changes in cortical polarization of the EEG lasting from 300 ms to several
115 seconds before the movements. Negative polarization have received different labels,
116 depending upon the experimental scenarios in which they were observed: MRCs or RPs
117 in preparation for voluntary movements, and CNV if it occurs between two consecutive

118 stimuli or responses [14]. Niazi et al. [15] as well as Lew et al. [16] have exploited, in
119 offline experiments, the RPs for the *prediction* of a forthcoming self-paced movement
120 66.6 ± 121 ms and 167 ± 68 ms before the action onset with an average maximum true
121 positive rate (TPR) of 82.5 ± 7.8 and 0.76 ± 0.07 , respectively. More recently, Xu et al.
122 showed the online *detection* of MRCPs with a TPR up to 0.79 [17]. However, the peak
123 of decoding performance is achieved about 300ms after the movement onset, unlike
124 our approach for the *prediction* of movement intention that works before the movement
125 onset.

126 Following the main goal of this study, we recorded EEG signals from 18 healthy
127 volunteers using a variation of the classical CNV paradigm in a simulated driving
128 experiment. In this study, we address the following questions: (i) Is it possible
129 to observe anticipatory related potentials during driving? Considering that, unlike
130 controlled psycho-physical experiments: driving task involves multitasking (upper and
131 lower limb movements) and the visual input is richer (including the moving stimuli
132 and other distractions). (ii) If this is the case, can these potentials be recognized in
133 single trials? (iii) We further investigate the possibility of detecting asynchronously the
134 movement intention with a moving window. To the best of our knowledge, no study has
135 been reported on the use of anticipatory brain potentials in order to detect movement
136 intention. How early could these potentials be detected in real-time?

137 The experiments and proposed methods are detailed in Section 2. Section 3 presents
138 the results of single-trial recognition of anticipation related potentials. Finally, we
139 discuss the results in Section 4, and suggest future directions in Section 5.

140 2. Materials and Methods

141 2.1. Experimental protocol and set-up

142 Eighteen healthy, right-handed subjects (2 female, average age 25.5 ± 4.1 yrs)
143 participated in the experiment. All had normal or corrected-to-normal vision and all
144 had an ample driving experience. The experimental protocols were approved by the
145 local ethical committee and subjects provided informed consent. Subjects sat in a car
146 simulator where a virtual roadway environment was displayed using the open source
147 *VDrift* software on the screen (experimental setup can be seen in Figure 1.a). The
148 participants were asked to drive the virtual car along a highway with soft turns, at a
149 speed of 100 Km/h, using the steering wheel, accelerate/brake pedals. There was no
150 other car on the virtual road. Visual cues were provided to the subjects at random
151 times indicating them to stop or resume their journey. The virtual environment was
152 shown on a projection screen for six of the subjects (see Figure 1.a: the size of the
153 screen was 100 inch and placed approximately 1.5 meter from the subject's seat). For
154 the remaining participants we used three 27 inch 3D monitors.

155 During the task one or more warning stimuli predicted the imperative stimulus
156 (see Figure 1.b and c). This design allowed us to test the difference between predictable

157 future events from the environment, some of them did not require the subjects to perform
158 an action (*No-go*), and imperative ones (*Go*). At a random time point during driving,
159 a visual cue appeared at the center of the screen showing a count-down from ‘4’ to
160 ‘1’, in seconds, followed by a text cue ‘Stop’. Upon this cue subjects were instructed
161 to immediately push the brake pedal. After a given period, a similar count-down of 4
162 seconds appeared, but this time it was followed by a ‘Start’ cue. Upon the onset of
163 this cue subjects had to push the acceleration pedal briskly. The interval between two
164 count-downs was drawn from a uniform distribution in the range of [10 20] s (mean and
165 standard deviation of 15 ± 2.87). In this paradigm, cues with numbers (‘4’, ‘3’, ‘2’,
166 ‘1’) corresponded to the warning stimuli, predicting the appearance of the imperative
167 stimulus (‘Start’/‘Stop’). The size of stimulus (0.1 rad) in the driver’s visual field was
168 similar for both setups (i.e. using the projection screen and the 3D monitors).

169 As can be seen in Figure 1.c, we defined two types of trials in our experiment:
170 *Drive* and *Brake* trials. The former comprises the time interval preceding the ‘Start’
171 cue, while the latter comprised the time interval before the ‘Stop’ cue. In both cases,
172 each trial contained three *No-go* epochs and one *Go* epoch, in terms of the classical *Go*
173 and *No-go* definition [7]. A *No-go* epoch is defined as the time interval between the
174 appearance of one number in the count-down to the next one, in which subjects were
175 not supposed to do any action after the cue. The time interval between cue ‘1’ and the
176 ‘Start/Stop’ cue, in which subjects were supposed to perform an action, is defined as a
177 *Go* epoch.

178 Each subject performed one experimental session composed of four runs of 15
179 minutes, each with resting periods of 5-10 min in between. Each session contained
180 an average of 91 ± 9.5 and 86 ± 9.5 trials for *Drive* and *Brake* trials, respectively.
181 During the *Drive* trials the car was stopped, and during the *Brake* trials, the car was
182 moving and subjects were continuously pressing the gas pedal fully. Therefore, the visual
183 information flow was richer in the *Brake* trials than in the *Drive* trials. Moreover, the
184 *Brake* trials required a different movement, switching from the gas pedal to the brake
185 pedal, while for *Drive* trials the subject only had to press the gas pedal. To reduce
186 EEG contamination due to movement artifacts, the subjects were instructed to fixate
187 a cross (size is around 0.02 rad) on the center of the screen to minimize facial or eye
188 movements during the appearance of the stimuli.

189 For 10 (out of 18) subjects we also provided their Reaction-time (RT) after the
190 *Brake* trials as a behavioral feedback. We hypothesized this feedback can help subjects
191 to better synchronize their actions (pressing the brake pedal) with the onset of the
192 imperative cue (‘Stop’). To summarize, we defined two sets of recordings, *Group1*
193 and *Group2*. *Group1* included the recordings of subjects S1-S9, in which no feedback
194 was provided to the subjects (S1-S6 with flat screen, S7-S9 with 3D screens). *Group2*
195 contained the recordings of subjects S10-S18, where the subjects received RT feedback
196 for the *Brake* trials (all subjects worked with 3D screens).

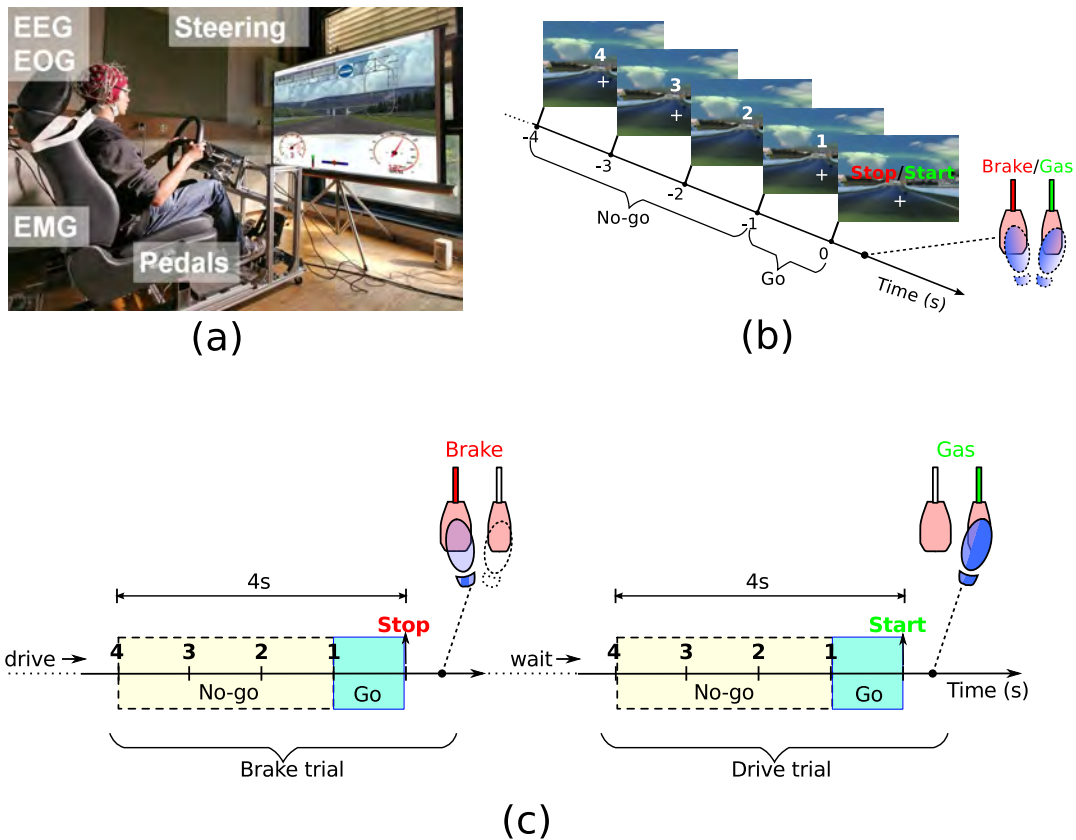


Figure 1. a) The experimental setup with the projection screen showing the virtual roadway environment and the car meters. b) Snapshots of the screen with the count-down stimuli. c) Time-line of the protocol: the first round of count-down stimuli followed by the ‘Stop’ cue to brake, waiting for around 15 seconds, and second round of count-down and ‘Start’ cue to accelerate. It corresponds to the two types of trials: *Brake* and *Drive* each containing one *Go* and three *No-go* epochs.

197 2.2. Data acquisition and preprocessing

198 The EEG was acquired using 64 electrodes arranged in the modified 10-20 international
 199 standard along with three EOG electrodes and two EMG electrodes using a Biosemi Inc
 200 ActiveTwo system. The EOG electrodes were placed above the nasion and below the
 201 outer canthi of the eyes, to derive horizontal, vertical and radial components. A pair of
 202 surface EMG electrodes were mounted on the *tibialis anterior* muscle of the subject’s
 203 right leg.

204 Event markers such as the triggers of the pedals (accelerate/brake) and steering, as
 205 well as the position of the car were provided by the car simulator at a sampling rate of
 206 256 Hz. Physiological signals (i.e. EEG, EMG, and EOG) were acquired at a sampling
 207 frequency of 2048 Hz, then down-sampled offline to 256 Hz and synchronized with the
 208 car simulator data.

209 The EEG data were spatially filtered by a common average reference (CAR) [18].
 210 Then, EEG was further filtered in the spatial domain using a weighted average filter
 211 (WAVG), as it has been shown to improve the classification performance of CNV

212 potentials [13]. WAVG can be seen as the opposite of the Laplacian filter, where the
 213 average neighboring activity is added, rather than subtracted. Given the value of the
 214 i^{th} electrode, $e_i^{CAR}(t)$ after CAR, WAVG returns $e(t) = e_i^{CAR}(t) + \frac{1}{K} \sum_j^K e_j^{CAR}(t)$, where,
 215 K represents the number of nearest neighbor electrodes considered. Afterwards, EEG
 216 was spectrally filtered by means of a non-causal narrow band-pass IIR filter (4th order,
 217 Butterworth) with cutoff frequencies between 0.1–1 Hz. EMG signals were rectified and
 218 then filtered with a bandpass Butterworth filter in the range of 20 to 50 Hz and smoothed
 219 with a moving average filter (window of 25 samples) [16]. EEG and EMG signals were
 220 segmented into *Go*, and *No-go* epochs (see Figure 1.c). The onset of the appearance of
 221 ‘Start/Stop’ cue on the screen is defined as time 0s. For each epoch (*Go* and *No-go*)
 222 the data were baseline corrected to the value of the sample at the onset of each cue.

223 2.3. Feature extraction and classification

224 2.3.1. Single trial classification

225 We evaluated the possibility of differentiating between *Go* and *No-go* epochs on a
 226 single-trial basis using well-known pattern recognition methods. We decoded activity at
 227 vortex (central-midline) where anticipation-related SCPs are most prominent [13]. For
 228 each epoch, the processed Cz potentials at 4 equally spaced time points (i.e. at -0.8 s, -
 229 0.6 s, -0.4 s, and -0.2 s) were used as a feature vector, $\mathbf{x} = [e_{Cz}(T_1) e_{Cz}(T_2) \dots e_{Cz}(T_4)] \in$
 230 R^4 where, T_k represents k^{th} time point. The choice for the number and timing of the
 231 features was based on previous studies from our group [13, 19]. In order to investigate
 232 the possibility of early detection, the proposed feature vector includes information only
 233 until 0.2 s before the onset of the imperative stimulus ‘Start’/‘Stop’.

234 For classification, we use the quadratic discriminant analysis (QDA) [20]. This
 235 choice was based on a preliminary evaluation where we compared, Linear discriminant
 236 analysis (LDA) and QDA and found that the latter yielded slightly higher classification
 237 performance [19]. We report here results using a 4-fold cross-validation method which
 238 maintain the chronological order of the data [21]; i.e each fold corresponds to a separate
 239 run.

240 The performance of the single trial classification was evaluated using the area under
 241 the curve (AUC) in the receiver operating characteristics (ROC) space [22]. ROC curves
 242 show the trade-off between the false positive rates (*FPR*) and true positive rates (*TPR*)
 243 of the classifier for different decision thresholds. In our case, *TPR* is the portion of *Go*
 244 epochs that are classified as *Go* and *FPR* is portion of *No-go* epochs detected as *Go*
 245 epochs. The results of this analysis are described in Section 3.2.

246 2.3.2. Movement intention detection

247 In order to evaluate the possibility of using anticipatory SCPs for predicting the
 248 driver’s movement intention, the performance of the classifier is tested in a moving
 249 window fashion. In this case, we pooled the data of *Drive* and *Brake* trials. It has
 250 been shown recently that there is a compromise between the value of the peak and its

251 timing [16, 23]. Therefore, four different models/classifiers were built using the features
252 extracted from a window of size 500 ms ending at different time points namely, at 200 ms
253 (w1), 300 ms (w2), 400 ms (w3), and 500 ms (w4), respectively before the onset of the
254 cues ‘3’, ‘2’, ‘1’, and ‘Start’/‘Stop’ (see Figure 2). Noting that, even though a smaller
255 window has been used for this study, we still kept the same number of features; 4 equally
256 spaced time points, in which the last one is the last time point of the window.

257 We tested the performance of these models using a sliding window with step of
258 62.5 ms, starting at 6 seconds before the onset of the imperative stimulus ‘Start’/‘Stop’
259 (2 second before the appearance of the first cue ‘4’) and ending at around 3 seconds after
260 the movement. The performance of the decoder was evaluated by the *Go* detection rate
261 (*GDR*), which is the percentage of the number of epochs, across all 4 folds, detected as
262 *Go*. *GDR* is considered as a measure of movement intention. The predictive power of
263 the decoder can be evaluated with the peak value of the *GDR* and the timing of the
264 peak. In order to evaluate the significance of our detector performance in detecting the
265 *Go* epochs, we generate a set of ‘random classifiers’ to estimate the ‘chance level’. For
266 that, we shuffle the training labels and perform 1000 times the 4-fold cross validation.
267 Therefore, the Null hypothesis is that the results of the original classification can be
268 drawn from a distribution generated by a set of random classifiers. If the classification
269 performance is out of the 95% of the distribution, we reject the Null hypothesis.

270 3. Results

271 3.1. Event-related potentials (ERP)

272 Figure 3.a shows the EEG grand averages across all subjects (N=18) for both the *Drive*
273 and *Brake* trials. The topographic plots of average scalp distribution show that the
274 negativity is spatially localized in the central area and is maximal at centro-medial
275 electrodes (especially Cz), which is consistent with existing literature on anticipation-
276 related SCPs [7, 13, 24]. Additionally, note that the subjects reacted using the right
277 foot, whose corresponding brain area is also under the same electrode [25].

278 In both *Drive* and *Brake* trials, we see a negative EEG deflection starting about 1
279 second before the appearance of the ‘Start/Stop’ cue; (i.e. around the onset of the last
280 warning stimulus (‘1’ cue)), and peaking at about 0 s which is the time of the appearance
281 of the ‘Start/Stop’ on the screen. In addition, a clear difference can be observed between
282 *Go* and *No-go* epochs (increasing negativity for *Go* and almost flat or slightly positive
283 response for all the other *No-go* epochs). The peak negativity is significantly higher for
284 *Brake* trials than *Drive* (t-test, $p < 0.01$), where the peak negativity is estimated as the
285 average of the potentials in individual trials from the window -200 ms to 0 s. The time
286 point 0 s corresponds to presentation of the imperative stimulus ‘Start’/‘Stop’.

287 Figure 3.b shows the grand averages of the EMG envelopes. The onset of increasing
288 activity in EMG is around -200 ms, confirming that there is no muscular activity of the
289 leg (*tibialis anterior* muscle) during the preparation phase. The horizontal line shows

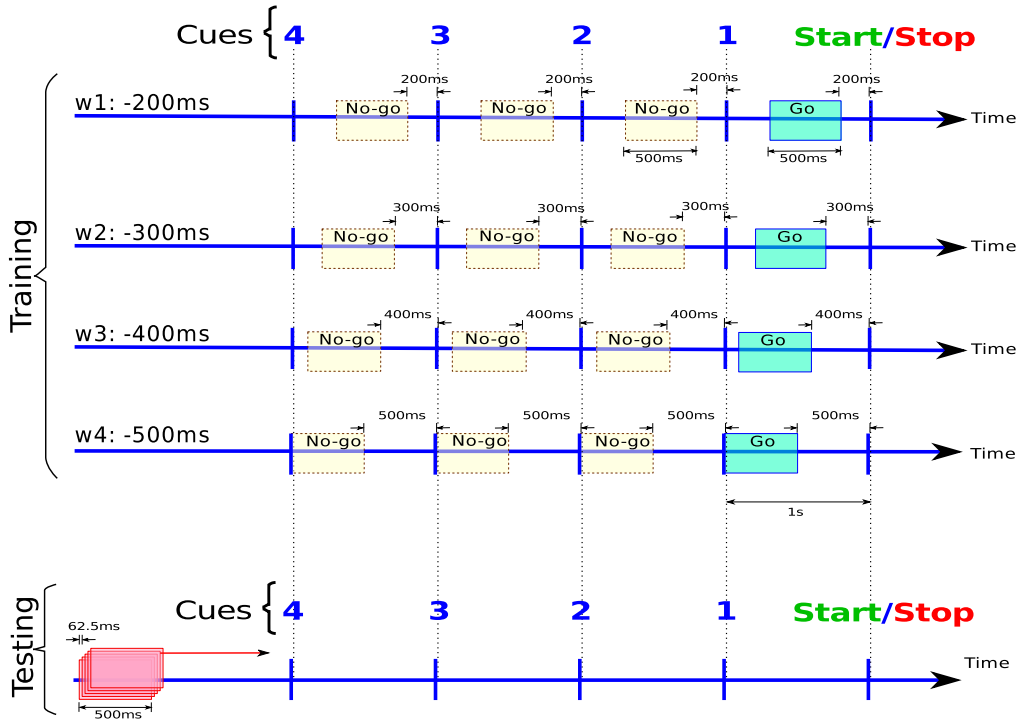


Figure 2. Training windows for the movement detection classifier. Four different models were built using the features extracted from a window of size 500 ms that ended at 200 ms (w1), 300 ms (w2), 400 ms (w3), and 500 ms (w4), respectively before the onset of the cues ('3', '2', '1', 'Start'/'Stop'). The segments that appeared before the warning stimulus were *No-go* epochs, whereas those appeared just before the imperative stimulus ('Start'/'Stop') were *Go* epochs. For testing (bottom trace), a similar window (500 ms) is used for extracting the features. Unlike the training phase, these windows were not time-locked but shifted with a step of 62.5 ms continuously.

290 the distribution of the timing of EMG onset for the *Drive* and *Brake* trials. This
 291 is defined as the time when the EMG activity exceeds a threshold equal to $\mu + 6\sigma$,
 292 where μ and σ are the mean and standard deviation of EMG signals of a one second
 293 window after the first warning cue (4) [26]. These results provide evidence that it is
 294 possible to observe anticipation-related EEG potentials during driving and before the
 295 muscular onset. As can be seen in Figure 3.a, a small negative deflection starting after
 296 the first warning stimulus ('4' cue) is also observed. The presence of a small negativity
 297 after the first warning stimulus and a relatively bigger negativity before the imperative
 298 stimulus (preceding the movement) is consistent with the bi-phasic negativity reported
 299 in previous studies on CNV potentials with a single pair of warning-imperative stimuli
 300 [7, 24].

301 3.2. Single trial classification

302 Figures 4 and 5 show the individual results of single-trial classification for *Brake* and
 303 *Drive* trials, respectively. The average AUC across subjects (N=18) is 0.83 ± 0.13 for
 304 *Brake* trials. A slight decrease in performance is observed for *Drive* trials with an

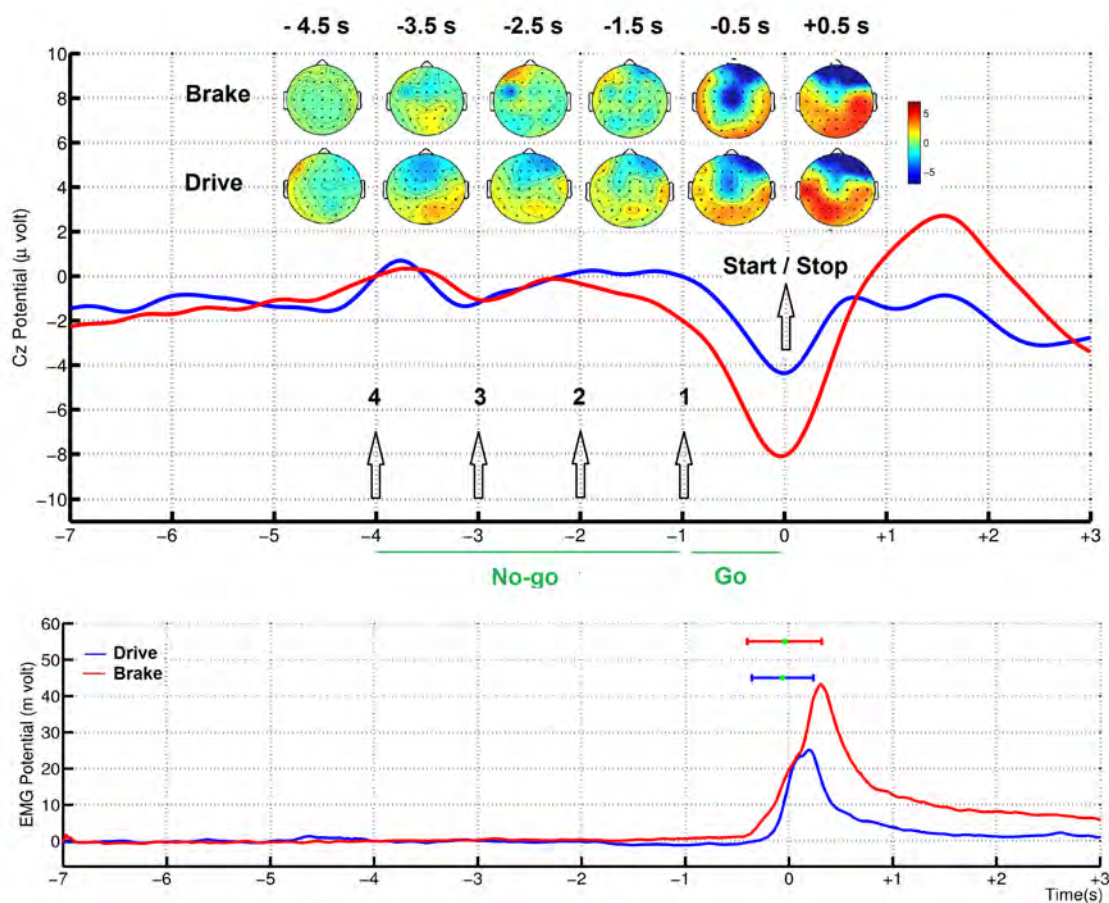


Figure 3. a) Anticipation-related SCPs. Top: Topographic representation of average EEG scalp distribution at different time points for *Drive* and *Brake* trials at 0.5 second before the onset of each cue which is shown by the arrow. Grand averages (N=18) of ERP for the Cz electrode, are shown in blue for *Drive* trials, in red for *Brake* trials. $t=0$ is the onset of the appearance of ‘Start/Stop’ cue and $t=-4$ is the onset of the appearance of the first count-down cue. b) Average of the envelope of the rectified EMG trace at *tibialis anterior* muscle to show the action execution. The horizontal line shows the distribution of the timing of EMG onset for *Drive* and *Brake* trials. The mean of of this distribution is shown with a green dot on top of each distribution. This figure is plotted using data of all subjects.

305 average AUC of 0.79 ± 0.12 (t-test, $p < 0.01$). Notably, 9 subjects reached an AUC above
 306 0.90 for *Brake* trials, and 5 subjects for *Drive* trials.

307 The average AUC of *Brake* trials for *Group1* is 0.82 ± 0.15 and for *Group2* is
 308 0.84 ± 0.13 (t-test, $p=0.59$). For *Drive* trials, the average AUC of *Group1* is 0.81 ± 0.10
 309 and for *Group2* is 0.76 ± 0.12 (t-test, $p=0.09$). The comparison between the classification
 310 performance of *Group2* and *Group1* shows that classification performance of *Brake* trials
 311 is higher than *Drive* trials for *Group2*; while for *Group1*, the classification performance
 312 of *Brake* trials is very similar to *Drive* trials. Interestingly, the difference between *Drive*
 313 and *Brake* trials is larger for *Group2* (The recordings with RT feedback for *Brake* trials).

314 The classification results reported in Figure 4 and 5 are based on features from
 315 a single electrode (Cz). We also tested whether classification performance improves
 316 when information from several electrodes is taken into account. To this end, we choose
 317 a Bayesian fusion technique at the level of classifiers [13]. Alternatively, the fusion
 318 could have been applied at the level of features (e.g. putting together the features
 319 of different EEG channels). However, the latter requires a larger amount of data due
 320 to the increased feature dimensionality. Figure 6 shows the classification results for
 321 different combinations of electrodes. The electrode configurations are chosen by the
 322 order of increased Euclidean distance from the Cz electrode location. As can be seen
 323 in the Figure 6, increasing the number of electrodes lead to very similar classification
 324 performance to just using the Cz electrode (The configuration with three electrodes on a
 325 vertical line resulted in slightly higher AUC than just using a single electrode. However,
 326 the difference is not statistically significant). Hence, these results suggest that a single
 327 classifier trained with single electrode data is sufficient for the single trial classification.
 328 This can potentially be due to the pre-processing using the WAVG spatial filter, which
 329 corresponds to a smoothing function that includes the information of the surrounding
 330 electrodes.

331 Having demonstrated the feasibility of differentiating between the *Go* and *No-*
 332 *go* conditions in single trials based on the activity of the electrode Cz for both
 333 types of events (*Drive* and *Brake*), we further analyzed the temporal behavior of the
 334 classification. To this end, as described in Section 2.3.2, we tested the classifiers using
 335 features computed from moving windows across time from the Cz electrode potentials.
 336 Note that for the purpose of detection of movement intention, we pooled the data of
 337 *Drive* and *Brake* trials. We tested four different classifiers -each trained on different
 338 windows with respect to the stimulus onset (w1-w4; c.f., Section 2.3.2)- on features
 339 extracted from moving windows starting from -6s till 3s, where 0s correspond to the
 340 appearance of imperative stimulus (i.e. ‘Start’/‘Stop’ cue) and $t=-4$ s is the onset of
 341 appearance of the first stimulus ‘4’ cue on the screen.

342 Figure 7 illustrates the results of the movement intention detection for each single
 343 subject using electrode Cz, and for the classification model trained based on the window
 344 w1 (ending at -200 ms before the stimuli). Each plot reports the average *Go detection*
 345 *rate (GDR)*, across the four test folds. Each point of the curve corresponds to the
 346 percentage of trials being detected as *Go* epoch, which we denote as a measure of
 347 movement intention at time t . The time points of the plot’s x-axis correspond to the
 348 latest sample of the moving window decoded by the classifier. The chance level for each
 349 time point is calculated by shuffling the labels of the training data and performing 1000
 350 times 4-fold cross validation (the mean of chance level in blue and the 95% confidence
 351 interval in blue shadow).

352 The *GDR* is above chance level for most participants (15 out of 18, except S5, S6,
 353 and S13) around the onset of the imperative stimulus. For all these participants, the
 354 *GDR* gradually raised above chance level and peaked earlier than the onset of imperative
 355 stimulus and the onset of movement. Interestingly, for most participants (e.g. S2) there

356 exist another peak on the *GDR* around -3s, which seem to signify detection of the early
 357 negativity of the CNV potential. Interestingly, we obtain low *GDR* values (except for
 358 S5, S6, and S15) in the periods of -6s to -4s and 1s to 3s, i.e. outside the windows
 359 used for training the classifier, suggesting the decoder has high specificity.

360 Figure 8 shows the peak *GDR* value for each window and its latency (the time
 361 when the highest performance is achieved) for the different training configurations (c.f.
 362 Figure 2). No statistical differences in the peak *GDR* were found across all training
 363 windows, what it is not the case for the latency (c.f., Figure 8). The earlier the training
 364 window, the earlier the *GDR* peak is detected. These results suggest that the movement
 365 intention can be detected based on the anticipation potentials as early as 320 ± 200 ms
 366 before movement with an average detection rate of 0.77 ± 0.12 .

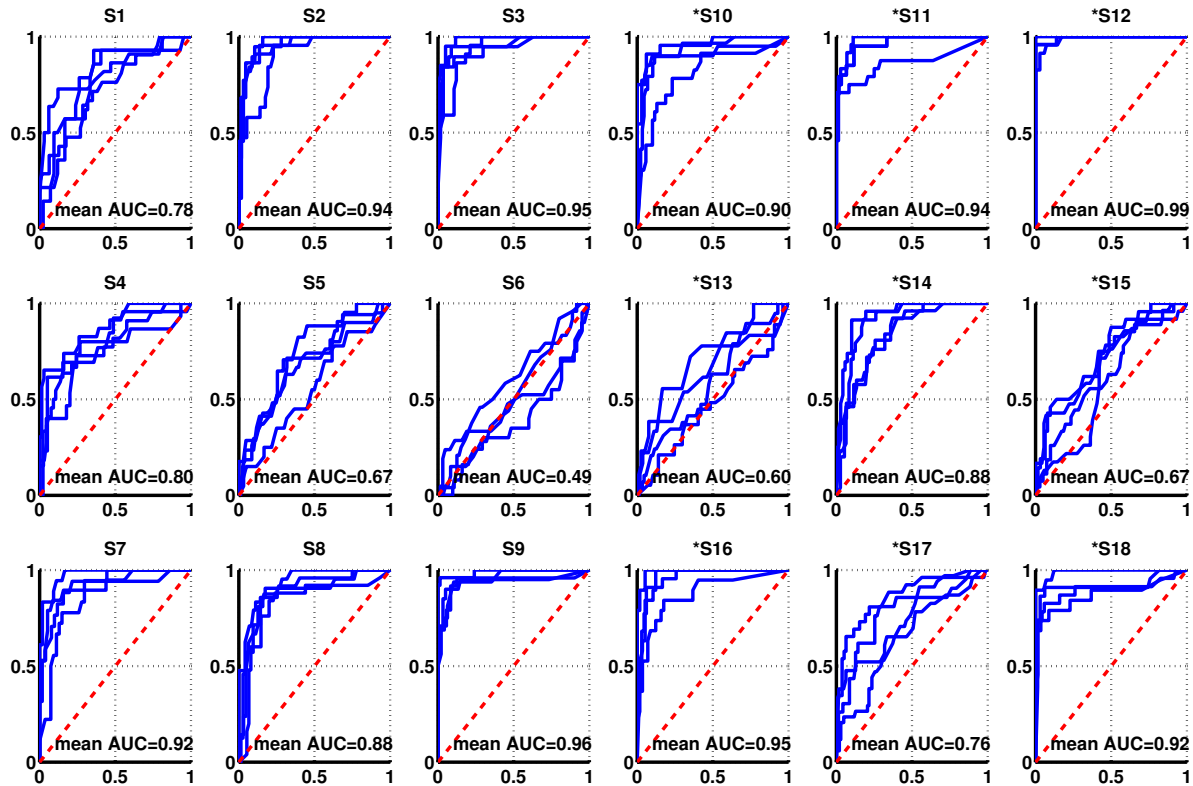


Figure 4. Individual classification performance for *Brake* trials. Subjects S1-S9, *Group 1*, did not receive RT feedback (S1-S6 with projection screen, S7-S9 with 3D screens), whereas subjects S10-S18, *Group 2*, with 3D screen and received RT feedback for the *Brake* trials. ROC curves and mean AUC values for all subjects (4-fold cross-validation). The dotted red line represents random performance and solid lines represents the ROC curves for each of the 4 folds. The mean AUC values are shown at the bottom of each ROC curve.

367 **4. Discussion**

368 In this study we investigated the existence of EEG correlates of anticipatory signals
 369 during driving. Firstly, the experiments conducted with 18 healthy participants shows
 370 that anticipatory event-related potentials, consistent with CNV signals reported in
 371 the literature [10, 11, 13], can be also observed in a simulated driving environment.
 372 Additionally, as can be seen in Figure 3.a, a small negative detection starting after the
 373 first warning stimulus ('4' cue) is also observed. The presence of a small negativity
 374 after the first warning stimulus and a relatively bigger negativity before the imperative
 375 stimulus (preceding the movement) is consistent with the bi-phasic negativity reported
 376 in previous studies with a single pair of warning-imperative stimuli [7, 24].

377 Secondly, although our experiments involve realistic settings—and not simple
 378 setups and stimuli as it is customary—, single-trial detection rates are promising. In the
 379 current experiment, the EEG signatures of anticipatory processes may be affected by
 380 visual distractors that naturally occur in driving tasks. Despite this, high performances
 381 up to an average AUC of 0.83 ± 0.13 for discrimination between the *Go* and *No-go* epochs

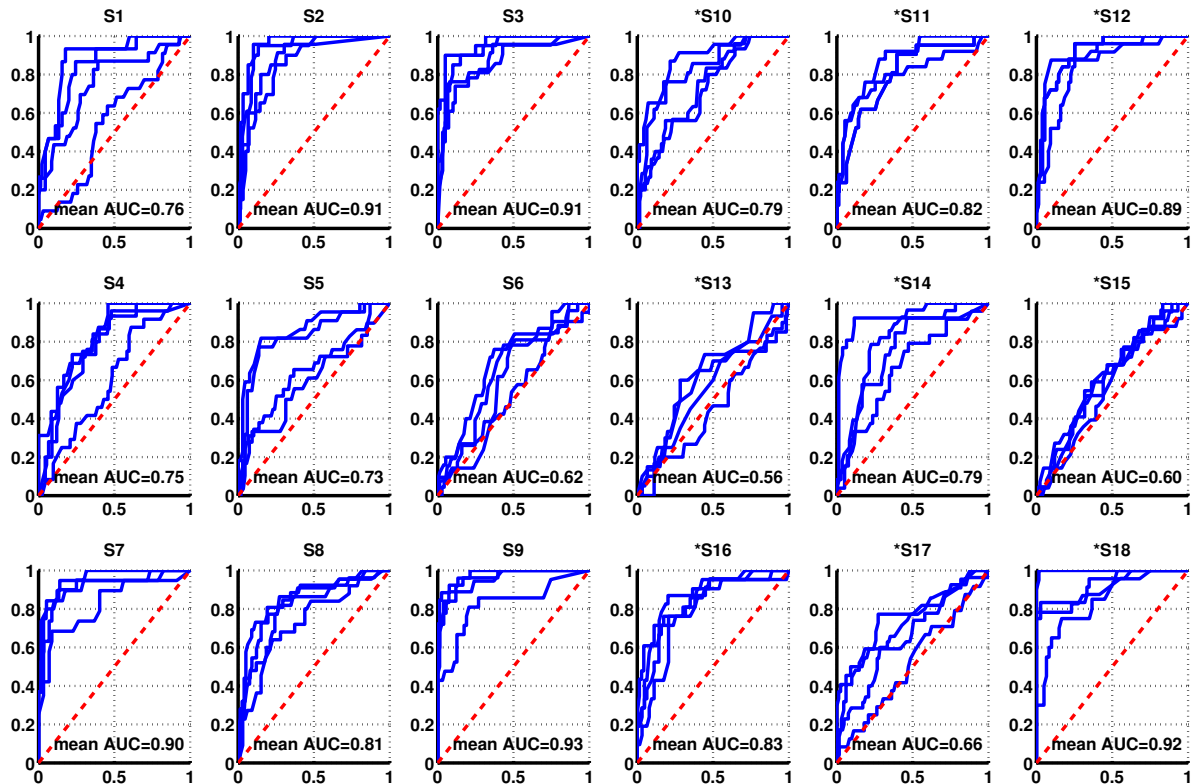


Figure 5. Individual classification performance for *Drive* trials. Subjects S1-S9, *Group 1*, did not receive RT feedback (S1-S6 with projection screen, S7-S9 used 3D screens), whereas subjects S10-S18, *Group 2*, used 3D screen and received RT feedback for the *Brake* trials. ROC curves and mean AUC values for all subjects (4-fold cross-validation). The dotted red line represents random performance and solid lines represent the ROC curves for each of the 4 folds. The mean AUC values are shown at the bottom of each ROC curve.

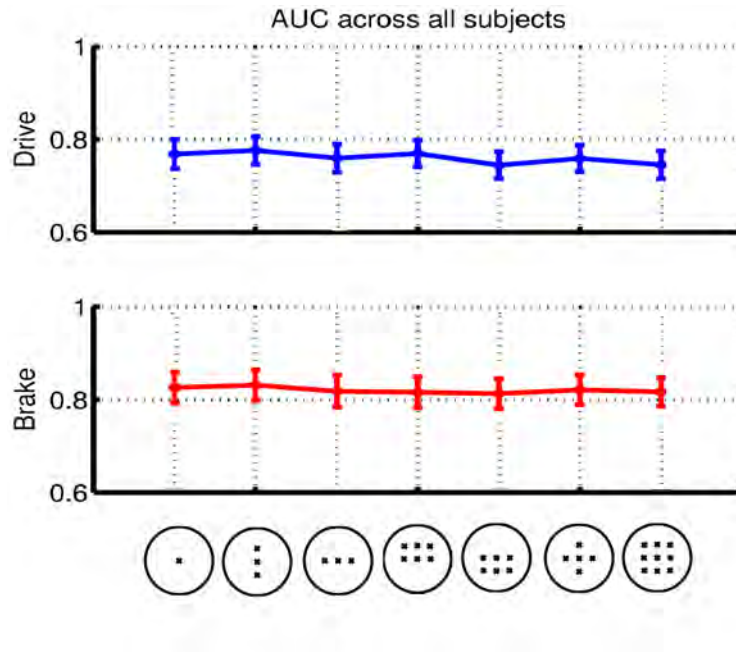


Figure 6. Average performance, AUC, across all subjects for different electrode configurations. The x-axis shows these electrode configurations in increasing the number of electrodes. The configuration with three electrodes on a vertical line resulted in slightly higher AUC than just using a single electrode. However, the difference is not statistically significant (t-test performed on the AUC values of *Drive* and *Brake* trials across 18 subjects)

382 for *Brake* trials have been achieved. We also observed a difference in the peak of the
 383 CNV potentials for the *Drive* and *Brake* trials. The *Brake* trials exhibit a larger negative
 384 peak, and classification results also show better performance compared to *Drive* trials
 385 (mean AUC of 0.79 ± 0.12). One possible explanation for these difference concerns the
 386 kind of movement that is performed in each case: for *Drive* trials, the subject waits for
 387 the ‘Go’ signal with the foot already placed on the gas pedal and just needs to push
 388 it, whereas, for the *Brake* trials the subject has to first release the gas pedal, move the
 389 foot to the brake pedal and then push it.

390 Thirdly, movement detection using the moving window shows that these
 391 anticipatory potentials can be detected as early as 320 ± 200 ms before the imperative
 392 stimulus with an average detection rate of 0.77 ± 0.12 across 18 participants. Our results
 393 of movement intention detection from CNV potentials are in in-line with previous
 394 work on the self-paced movement intention detection [23, 15, 16]. Remarkably, we
 395 demonstrate low *GDR* values in the normal driving intervals (-6 s to -4 s and 1 s to 3 s),
 396 clearly outside the period of appearance of cues which is used for training. Such high
 397 specificity across time may be beneficial for online application.

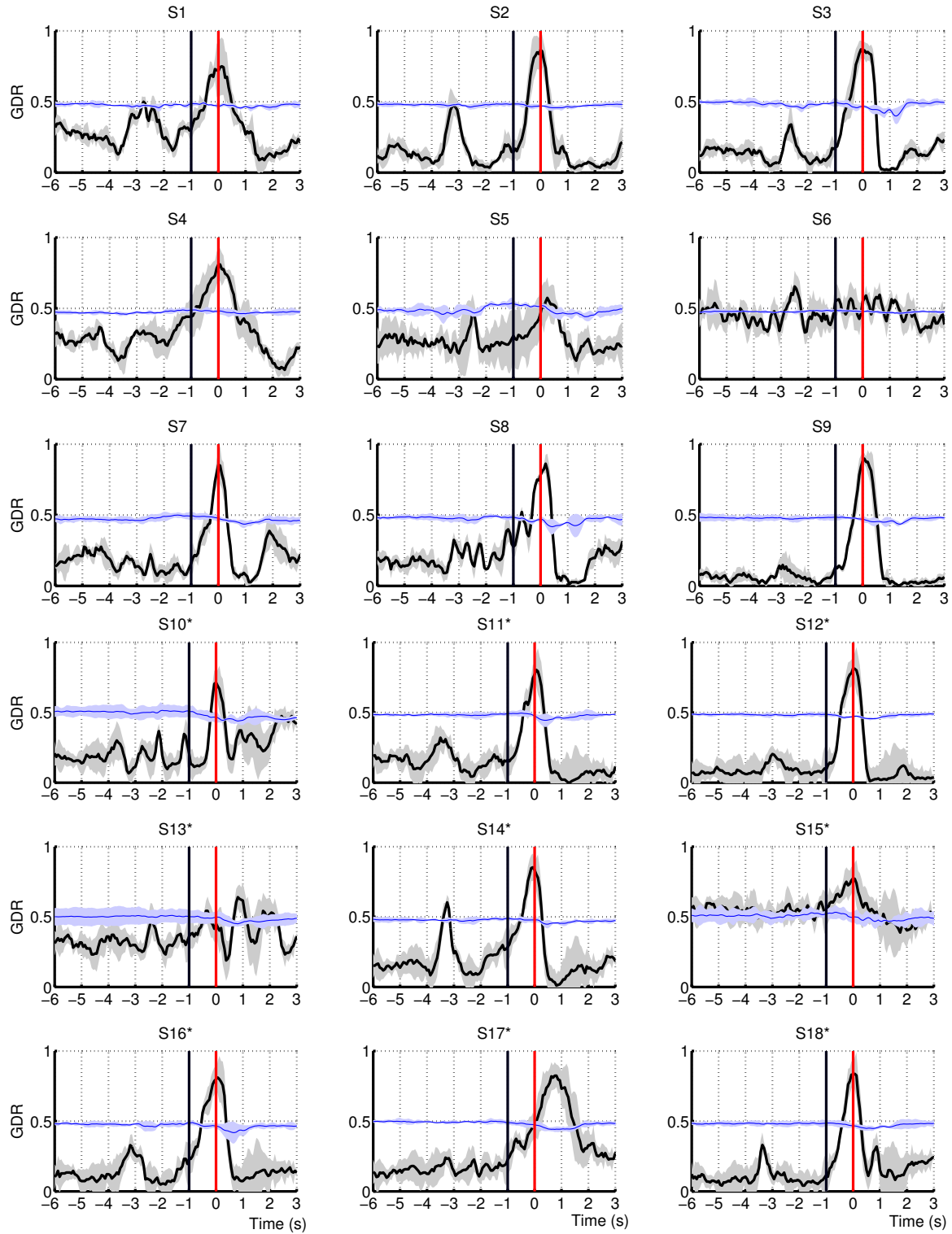


Figure 7. The results of movement intention detection through the *Go detection rate* (*GDR*) measure for all subjects. Classification performance is estimated using the training window ending -200 ms (w_1) and testing during the time interval $[-6, +3]$ s. The shaded region surrounding the average *GDR* illustrates the standard deviation at each point. The vertical red line in red color refers to the onset of the imperative stimulus; ‘Start/Stop’. The black vertical line corresponds to the onset of the last warning stimulus. The chance level for each time point is calculated by shuffling the labels of the training data and performing 1000 times 4-fold cross validation (the mean of chance level in blue and the 95% confidence interval in blue shadow).

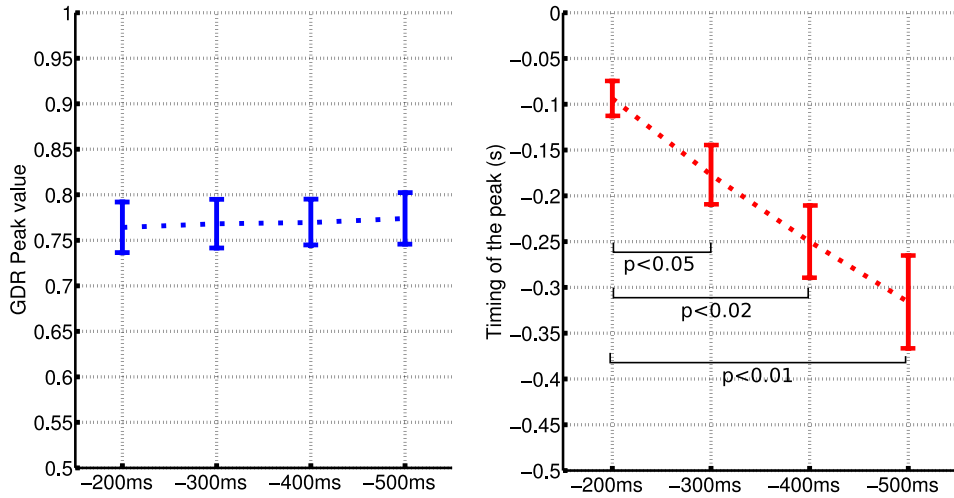


Figure 8. Performance of classifiers trained on different windows: on the left, the peak detection rates are indicated and on the right, the timing of the peak detection rates for various training windows (w1: 200 ms, w2: 300 ms, w3: 400 ms, w4: 500 ms). No statistical differences in the peak *GDR* were found across all training windows, what it is not the case for the latency. The earlier the training window, the earlier the *GDR* peak is detected.

398 5. Conclusions and Future works

399 This study presents and demonstrates the possibility of discriminating the anticipation-
 400 related potentials and predicting movement onset from scalp EEG during simulated car
 401 driving. It is worth noting that during the experiment, the subjects needed to process
 402 changing visual inputs. The immediate future step, before testing our methods in a real
 403 car, is to conduct online experiments with more realistic driving scenarios (real traffic
 404 lights, inclusion of other vehicles) to assess the real-time detection of anticipatory signals.
 405 Complementary to other approaches for the early detection of movement onset or
 406 intention to move by means of various EEG correlates appearing in self-paced movement
 407 tasks [15, 17, 16], we are the first, to the best of our knowledge, to prove the possibility
 408 of predicting the subject's voluntary intention in response to external events during
 409 driving (e.g. the count-down warning cues resemble the traffic lights in real driving) by
 410 means of detecting anticipatory brain potentials. This approach also complements other
 411 efforts on decoding neural correlates during driving tasks, in particular, the recent study
 412 on the detection of the intention of emergency braking [4, 5, 6]. Our results support
 413 the feasibility of BCI systems for future cars in order to predict the driver's movement
 414 intentions. Predicting the driver's will can be beneficial as the driving assistance system
 415 will be aligned with the driver's intention. Thus, in the scenario of the traffic lights
 416 described in this paper, the driving assistance system can exploit the BCI output to
 417 provide support as follows. In the case that the driver is not aware of the traffic light
 418 changing colors, no anticipatory brain potentials are generated and the BCI detects no
 419 intention to execute a movement. The driving assistant could then provide a warning

420 to the driver who would have time to brake by himself, preventing the car to generate
421 an emergency brake at the last moment that may cause him a negative surprise. On the
422 other hand, detecting the planned action before its execution also brings advantages as
423 it enhances the driver's experience: it will ensure a seamless interaction between the car
424 and the driver, promoting the car to behave as a truly extension of driver's body.

425 6. Acknowledgement

426 The work was supported by Nissan Motor Co. Ltd., under the 'Research on Brain
427 Machine Interface for Drivers'. The authors would like to thank Gangadhar Garipelli,
428 Huaijian Zhang, and Serafeim Perdakis for their valuable comments and help with the
429 design of the experimental protocol, as well as valuable discussions regarding the analysis
430 and proofreading.

431 References

- 432 [1] C. H. Chuang, P. C. Lai, L. W. Ko, B. C. Kuo, and C. T. Lin, "Driver's cognitive state
433 classification toward brain computer interface via using a generalized and supervised technology,"
434 in *International Joint Conference on Neural Networks*, 2010, pp. 1–7.
- 435 [2] F. C. Lin, L. W. Ko, S. Chen, C. Chen, and C. Lin, "EEG-based cognitive state monitoring and
436 prediction by using the self-constructing neural fuzzy system," in *International Symposium on
437 Circuits and Systems*, 2010, pp. 2287–2290.
- 438 [3] C. Dijksterhuis, D. de Waard, K. Brookhuis, B. Mulder, and R. de Jong, "Classifying visuomotor
439 workload in a driving simulator using subject specific spatial brain patterns." *Frontiers in
440 Neuroscience*, vol. 7, no. 149, 2013.
- 441 [4] S. Haufe, M. S. Treder, M. F. Gugler, M. Sagebaum, G. Curio, and B. Blankertz, "EEG potentials
442 predict upcoming emergency brakings during simulated driving," *Journal of Neural Engineering*,
443 vol. 8, no. 5, pp. 1–11, 2011.
- 444 [5] S. Haufe, J. Kim, I. H. Kim, A. Sonnleitner, M. Schrauf, G. Curio, and B. Blankertz,
445 "Electrophysiology-based detection of emergency braking intention in real-world driving,"
446 *Journal of Neural Engineering*, vol. 11, no. 5, p. 056011, 2014.
- 447 [6] I. H. Kim, J. W. Kim, S. Haufe, and S. W. Lee, "Detection of braking intention in diverse situations
448 during simulated driving based on EEG feature combination," *Journal of Neural Engineering*,
449 vol. 12, no. 1, p. 016001, 2015.
- 450 [7] W. G. Walter, R. Cooper, V. J. Aldridge, and W. C. Mccallum, "Contingent negative variation :
451 An electric sign of sensorimotor association and expectancy in the human brain," *Nature*, vol.
452 203, pp. 380–384, 1964.
- 453 [8] R. De Charette and F. Nashashibi, "Real time visual traffic lights recognition based on spot light
454 detection and adaptive traffic lights templates," in *IEEE Intelligent Vehicles Symposium*, 2009,
455 pp. 358–363.
- 456 [9] M. Omachi and S. Omachi, "Traffic light detection with color and edge information," in *2nd IEEE
457 International Conference on Computer Science and Information Technology*. IEEE, 2009, pp.
458 284–287.
- 459 [10] W. Kirsch and E. Hennighausen, "ERP correlates of linear hand movements: Distance dependent
460 changes." *Clinical Neurophysiology*, vol. 121, pp. 1285–1292, 2010.
- 461 [11] P. Kropp, A. Kiewitt, H. Gbel, P. Vetter, and W. Gerber, "Reliability and stability of contingent
462 negative variation." *Applied Psychophysiology and Biofeedback*, vol. 25, no. 1, pp. 33–41, 2000.
- 463 [12] R. Chavarriaga, X. Perrin, R. Siegwart, and J. d. R. Millán, "Anticipation and error-related EEG

- 464 signals during realistic human-machine interaction: A study on visual and tactile feedback,”
465 *34th International Conference of the IEEE Engineering in Medicine and Biology Society*, 2012.
- 466 [13] G. Garipelli, R. Chavarriaga, and J. d. R. Millán, “Single trial analysis of slow cortical potentials:
467 a study on anticipation related potentials,” *Journal of Neural Engineering*, vol. 10, p. 036014,
468 2013.
- 469 [14] N. Birbaumer, T. Elbert, A. G. Canavan, and B. Rockstroh, “Slow potentials of the cerebral cortex
470 and behavior,” *Physiological Reviews*, vol. 70, pp. 1–41, 1990.
- 471 [15] I. Niazi, N. Jiang, O. Tiberghien, J. Nielsen, K. Dremstrup, and D. Farina, “Detection of movement
472 intention from single-trial movement-related cortical potentials,” *Journal of Neural Engineering*,
473 vol. 8, p. 066009, 2011.
- 474 [16] E. Lew, R. Chavarriaga, S. Silvoni, and J. d. R. Millán, “Detection of self-paced reaching movement
475 intention from EEG signals,” *Frontiers in Neuroengineering*, vol. 5, p. 13, 2012.
- 476 [17] R. Xu, N. Jiang, C. Lin, N. Mrachacz-Kersting, K. Dremstrup, and D. Farina, “Enhanced
477 low latency detection of motor intention from EEG for closed loop brain computer interface
478 applications,” *IEEE Transactions on Biomedical Engineering*, vol. 61, no. 2, pp. 288–296, 2014.
- 479 [18] D. J. McFarland, L. M. McCane, S. V. David, and J. R. Wolpaw, “Spatial filter selection for EEG-
480 based communication,” *Electroencephalography and Clinical Neurophysiology*, vol. 103, no. 3,
481 pp. 386–394, 1997.
- 482 [19] Z. Khaliliardali, R. Chavarriaga, L. A. Gheorghe, and J. d. R. Millán, “Detection of Anticipatory
483 Brain Potentials during Car Driving,” in *34th Annual International Conference of the IEEE
484 Engineering in Medicine and Biology Society*, 2012, pp. 3829–3832.
- 485 [20] R. O. Duda, P. E. Hart, and D. G. Stork, *Pattern Classification*, 2nd ed. New York: Wiley, 2001.
- 486 [21] N. Bourdaud, R. Chavarriaga, F. Galán, and J. d. R. Millán, “Characterizing the EEG correlates of
487 exploratory behavior,” *IEEE Transactions on Neural Systems and Rehabilitation Engineering*,
488 vol. 16, no. 6, pp. 549–556, 2008.
- 489 [22] T. Fawcett, “An introduction to ROC analysis,” *Pattern recognition letters*, vol. 27, no. 8, pp.
490 861–874, 2006.
- 491 [23] L. Gheorghe, R. Chavarriaga, and J. d. R. Millán, “Steering timing prediction in a driving simulator
492 task,” in *35th Annual International Conference of the IEEE Engineering in Medicine and Biology
493 Society*, 2013, pp. 6913–6916.
- 494 [24] N. Loveless and A. Sanford, “The impact of warning signal intensity on reaction time and
495 components of the contingent negative variation.” *Biological Psychology*, vol. 2, no. 3, p. 217,
496 1975.
- 497 [25] G. Pfurtscheller, C. Neuper, C. Andrew, and G. Edlinger, “Foot and hand area mu rhythms,”
498 *International Journal of Psychophysiology*, vol. 26, no. 1-3, pp. 121–135, 1997.
- 499 [26] D. Bilt and D. Glas, “Detection of onset and termination of muscle activity in surface
500 electromyograms,” *Journal of Oral Rehabilitation*, vol. 25, no. 5, pp. 365–369, 1998.